To be submitted to
Lettere Nuovo Cimento

G. P. Capitani, E. De Sanctis, S. Faini, C. Guaraldo, G. Ricco, M. Sanzone, A. Zucchiatti and R. Scrimaglio : FIRST MEASUREMENTS OF THE ENERGY SPECTRA OF THE LEALE PHOTON BEAM.

G. P. Capitani, E. De Sanctis, S. Faini, C. Guaraldo, G. Ricco[(x)], M. Sanzone[(x)], A. Zucchiatti[(x)] and R. Scrimaglio: FIRST MEASUREMENTS OF THE ENERGY SPECTRA OF THE LEALE PHOTON BEAM.

Positron annihilation in flight has been widely used in recent years to obtain quasi monochromatic photon beams with variable energy. The main features of the existing facilities, in similar angular acceptance conditions, are reported in Table I. In most cases the design has been limited to low peak energies (below 100 MeV) and to collection angles in the very forward direction.

At higher energies a very poor monochromatic contribution in the forward direction is obtained due to the wide angular distribution of the annihilation spectrum and to the forward peaked bremsstrahlung. Large collection angles with respect to the positron direction must therefore be used at the expenses of the total intensity and of the resolution.

On the other side, bremsstrahlung experiments have recently pointed out a remarkable physical interest in photonuclear reactions at the energies above 100 MeV in order to investigate short range interactions[(6)] and pionic effects in nuclear structure[(7)].

In this report we present the preliminary results on the energy spectra, taken at 200 MeV positron energy of the Frascati linac, of the new monochromatic photon beam obtained at the LEALE Laboratory. The end point energy of this beam can be continuously varied from 80 MeV up to 300 MeV.

The beam transport system has already been described in detail in ref. (8) and is partially reported in Fig. 1. The beam energy is selected by a system of two tantalum slits, S, 15 mm thick each, positioned in the symmetry plane of a four magnet system (BM_1, BM_2, BM_3, BM_4) which gives a Penner type achromatic deflection. The slits have been calibrated in

(x) - G. Ricco, M. Sanzone and A. Zucchiatti - Istituto di Scienze Fisiche dell'Università di Genova, and Sezione INFN di Genova.

TABLE I

Laboratory	Annihilation target (rad.lengths)	E_γ (MeV)	N_γ (s^{-1})	$\Delta E_\gamma / E_\gamma$ %	Collection angle (mrd)	Angular acceptance (mrd)
Saclay I[1]	Li (0.002)	30	2.10^4	2.00	0	26,4
NBS[4]	H Li	40		3.7		
Giessen[15]	Be (0.002)	8-40	2.10^4	1.3	0	9.6
Livermore[2,4]	Be	10-70	10^4	.25	0	
Saclay II[3]	H Li (0.002)	30-90	6.10^4	2.0	35	0.76
Mainz[4]		10-100		1.0		
Orsay[5]	H Li (0.01)	250-500	10^5	7.0	23.9	2.8
Frascati	H (0.011)	80-300	2.10^6 2.10^5	1.0 10.0	0 17.0	1.0 1.0

energy by comparison with the positron spectrum measured by a system of secondary emission monitors in the focal plane of an analysing magnet at the end of the linac[9]. The beam spot, as observed on a plastic scintillator screen, V, which can be inserted at the end of the vacuum pipe, has ellipti cal shape with semiaxes 7 mm and 5 mm long respectively. In order to get a precise definition of the photon emission angle, a very accurate alignment of the positron beam along the optical axis is required. This is achieved op timizing on the positron monitors the beam intensity after two removable copper collimators, F_1 and F_2 (ϕ = 7 mm and 6 mm respectively) by two pairs of steering coils. The final quadrupole doublet, Q_1 and Q_2, normally turned off, is only used to test the correct alignment, verifying on the scintillator screen V the absence of beam steering effects.

The intensity of the positron beam along the transport channel is continuously monitored by a toroidal charge monitoring system, M. The beam induced signal is compared with a standard current calibration pulse and integrated to give the total charge[10]. After the annihilation target, the positrons are deflected by the damping magnet, SM_1, into a shielded Faraday cup, used as a beam catcher (Fig. 2). The Faraday cup signal, integrated by a standard current digitizer (ORTEC 439), provides an absolute charge monitor.

The positron spectrum at 200 MeV, as transmitted by the transport system without any energy definition, is reported in Fig. 3. The beam average current at 50 Hz and $1.5 \ 10^{-4}$ duty ratio is ~ 20 nA. The F. W. H. M. turns out to be 1.5%.

Positrons annihilate in a cylindrical liquid Hydrogen target (ϕ = = 55 mm) 0.011 radiation lengths thick . The photons have been collected at two different angles: θ_1 = 0.0 $\pm$ .5 mrd and θ_2 = 17.5 $\pm$ 0.5 mrd, by a set of five lead collimators C_1, C_2, C_3, C_4 and C_5 (Fig. 4a) followed by three small sweeping magnets (SM_2, SM_3, SM_4). Beam monitoring has been
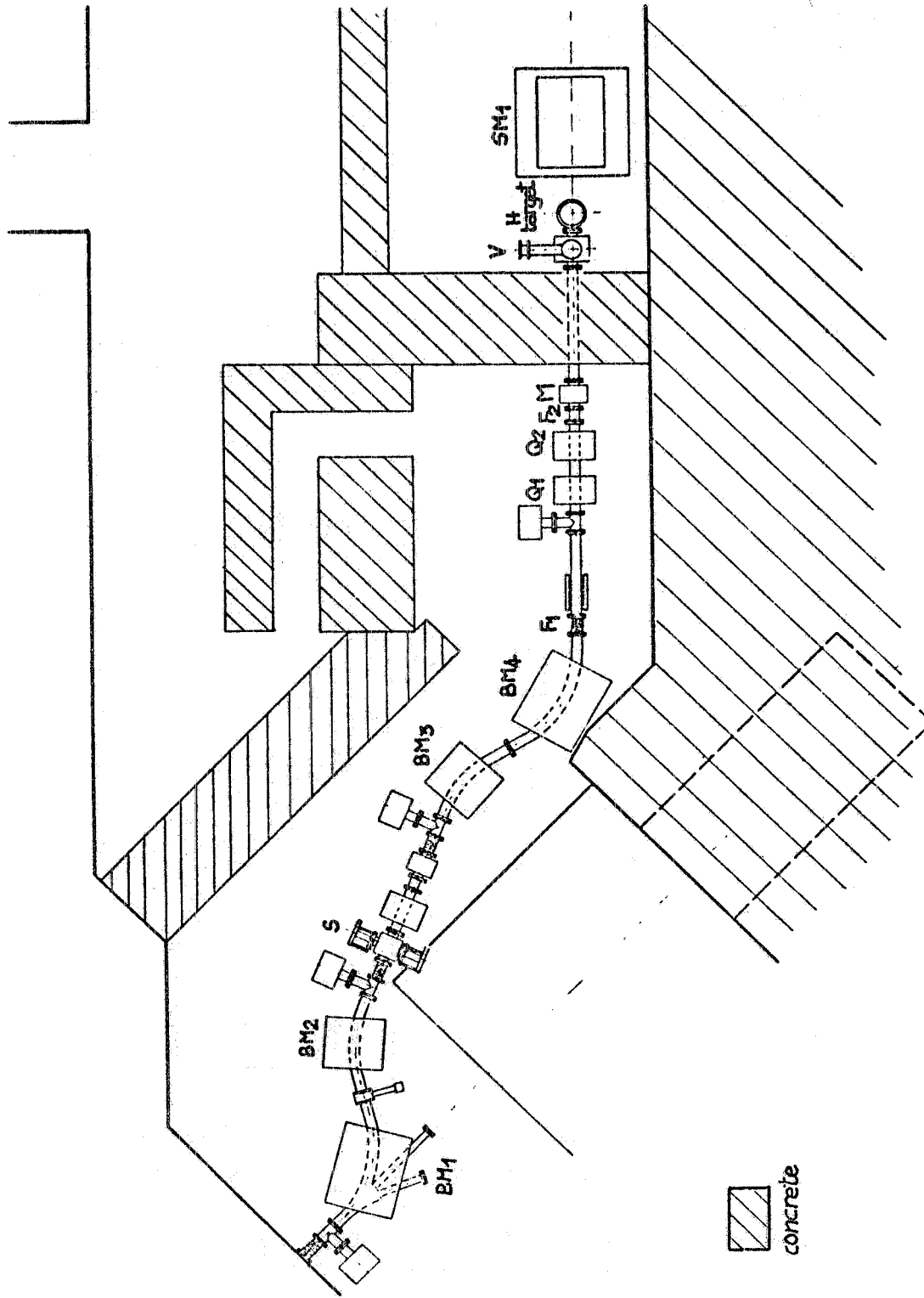
FIG. 1 - Layout of the positron beam transport system: BM_1, BM_2, BM_3, BM_4 = bending magnets; S = energy defining slits; F_1, F_2 = copper collimators; Q_1, Q_2 = quadrupoles; V = beam visualizer; SM_1 = damping magnet; M = toroidal monitor.
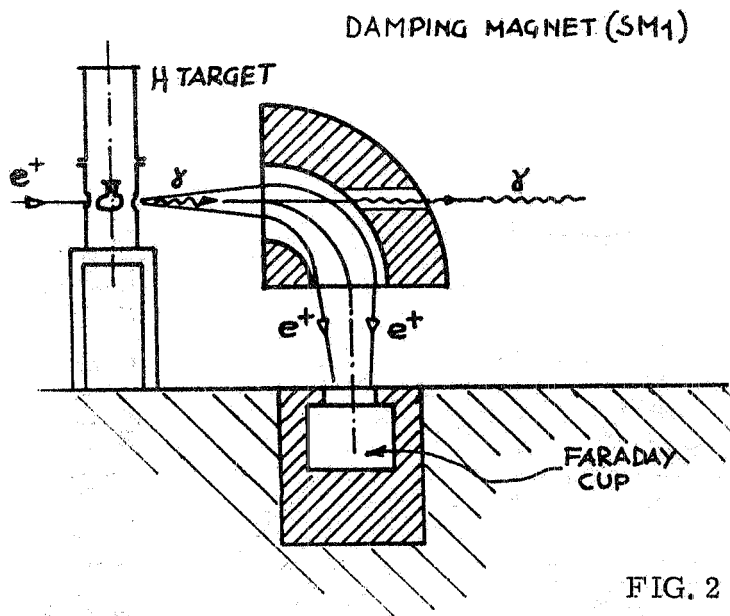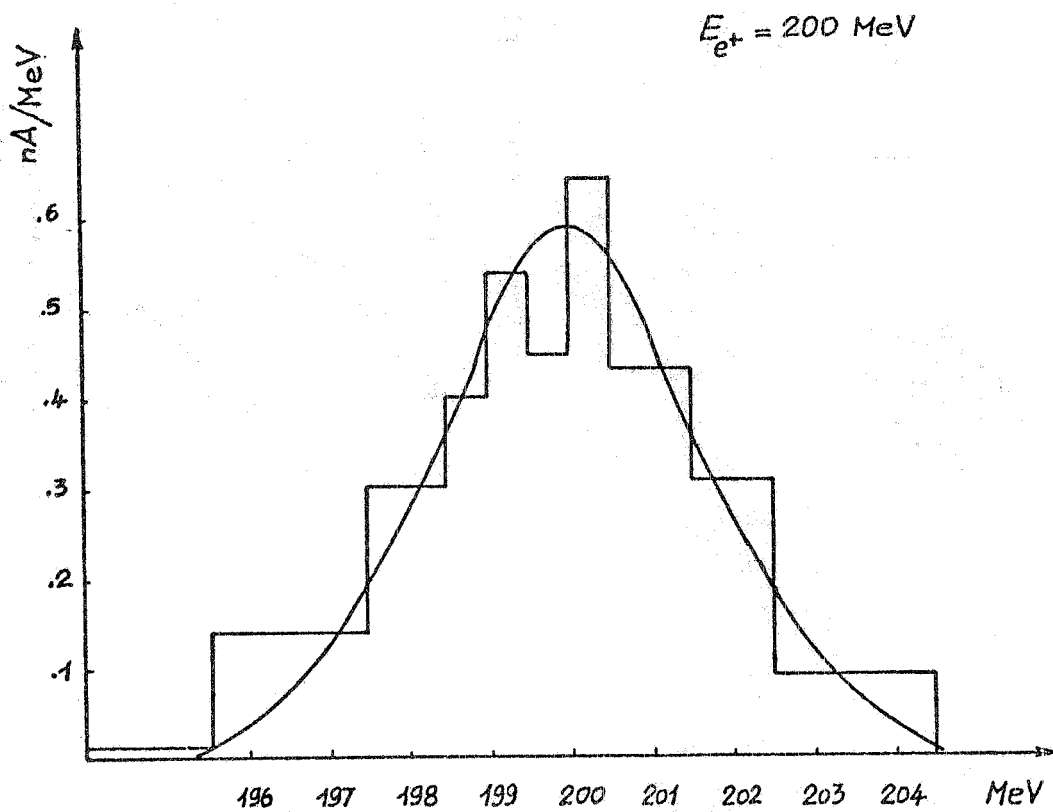
4.

FIG. 2 - Positron beam catcher.

FIG. 3 - Positron energy spectrum: the istogram is obtained at the end of the linac; the solid line is obtained at the annihilation target point.

performed by a standard NBS P2 chamber; some comparison measurements have also been taken by a Komar type quantameter[11] with equivalent results. During the measurements care has been taken to keep stable the ratio between positron and photon intensities.

The photon spectrum has been measured using an available pair spectrometer[12], schematically shown in Fig.4b) with flat rectangular poles (size 20x30 cm^2) and a gap 1.5 cm high. The magnet small gap and optical properties limit the photon collimation angle to $\sim 8 \cdot 10^{-6}$ srd. A Hall probe, permanently inserted at a fixed position between the poles, enables the continuous testing of the magnetic field value with $1\%_0$ accuracy.

Electron-positron pairs are created in a variable thickness Aluminum converter. The pairs are deflected of $19°$ and detected in coincidence by a system of scintillation counters. In the electron arm, five energy channels are defined by five scintillation counters $E_1 \div E_5$ (1 cm wide, 2 cm thick and 10 cm high each) in coincidence with the two large scintillators E_6, E_7 (20 x 1 x 20 cm^3) in order to decrease the background. In the positron arm, only one energy is selected by the coincidence between the scintillation counters P_1 (0.6 x 2 x 10 cm^3) and P_2 (2 x 0.6 x 10 cm^3) (Fig. 4b). Γ

The block diagram of the electronics is shown in Fig. 5. Random coincidences have been measured with a similar electronics set up.

In Figs. 6a and 7a the photon spectra obtained at the positron energy of 200 MeV are reported. Data at $\theta_1 = 17.5$ mrad have been collected using pair converters of two different thicknesses (0.4 mm and 0.8 mm). The measurement at $\theta_2 = 0$. mrad has been performed with a 0.06 mm thick converter, in order to reduce the multiple scattering effects.

Both the spectra show a peak at the correct annihilation energy with a bremsstrahlung continuous tail. The annihilation-bremsstrahlung ratio as well as the peak resolution are very sensitive to the collection angle.

Different background sources have been accurately investigated:

a) annihilation target off background: the counting rate is then mainly due to the bremsstrahlung contribution from the 0.1 mm thick Al window at the exit of the pipe line and from the 1.0 m air path between the exit window and the damping magnet SM_1. This background amounts to about 30% at $0°$ and 7% at $1°$ of the total observed counting rate in the bremsstrahlung region. An extension of the vacuum pipe, at present in progress, will reduce this background of 2/3;

b) pair converter off background with the H annihilator on the beam. This contribution has turned out to be completely negligible;

c) random coincidences between the positron and electron arms: the energy spectrum is flat and amounts to $\sim 25\%$ of the average bremsstrahlung contribution in the tail region.

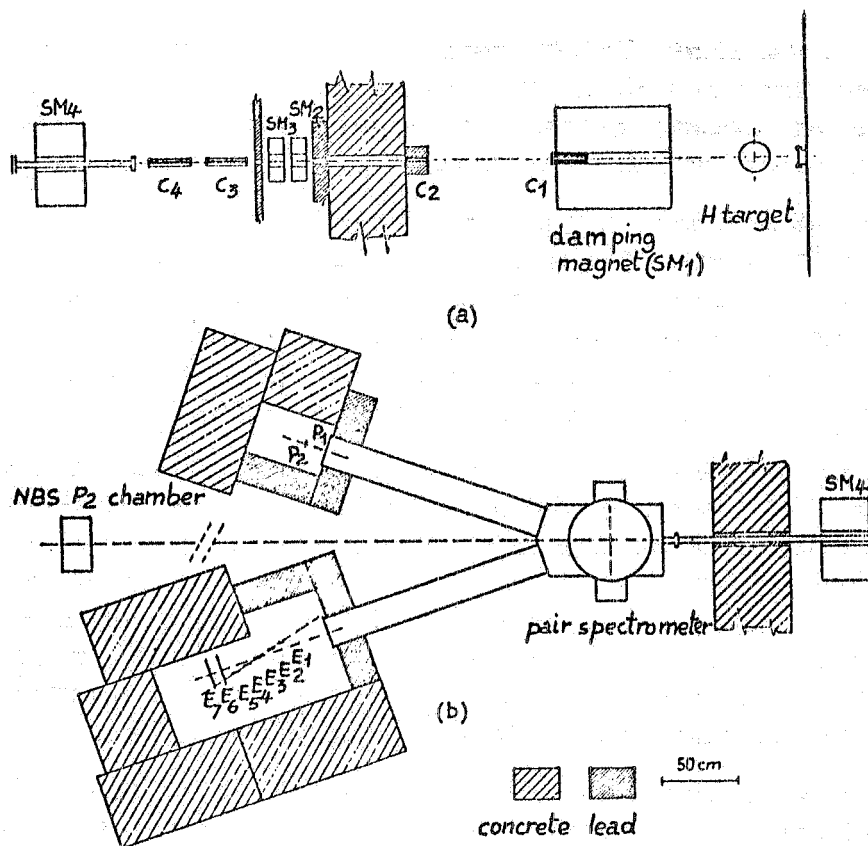In Figs. 6 and 7 the total background has been subtracted; the large

FIG. 4 - a) Layout of the photon beam collecting system (C_1, C_2, C_3, C_4 = lead collimators; b) experimental set up.
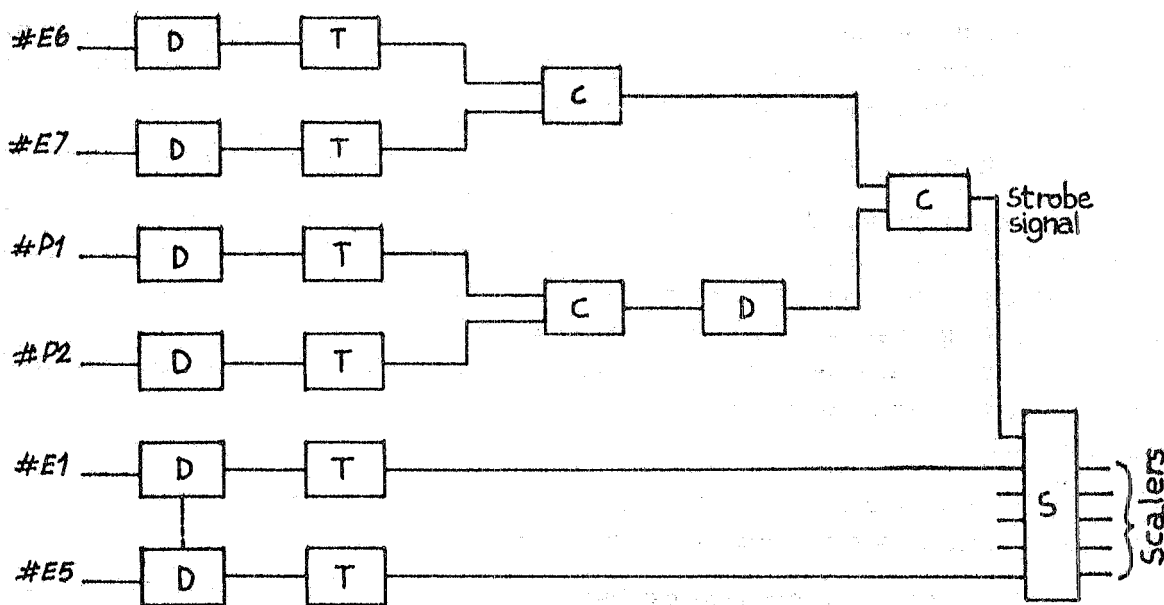

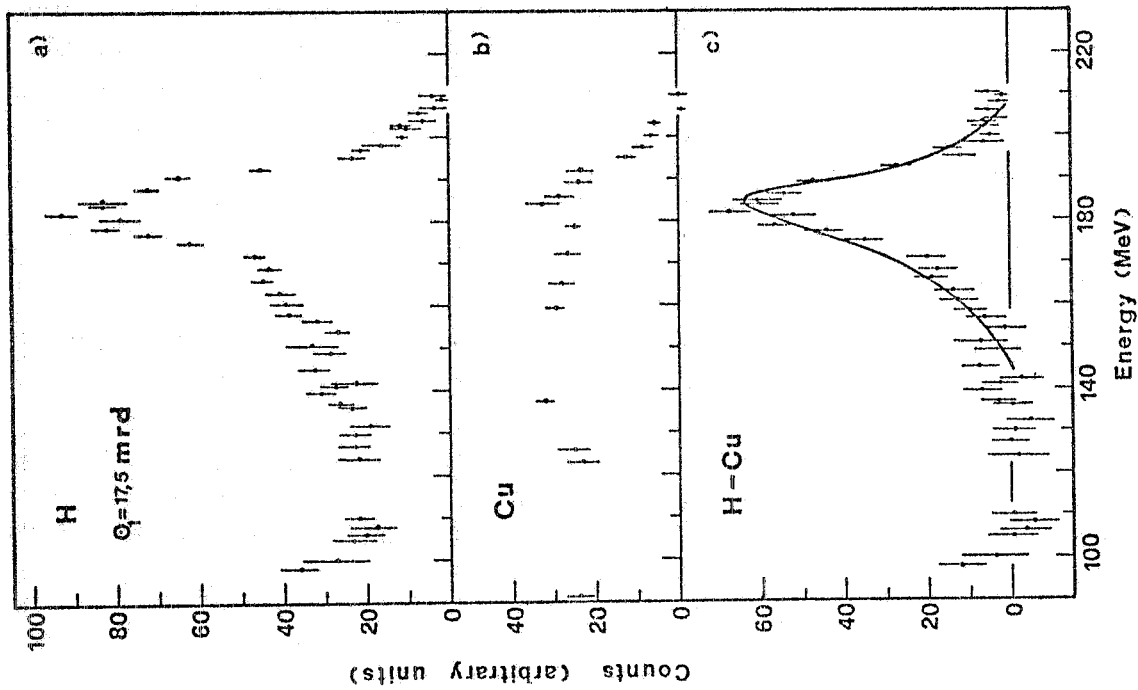FIG. 5 - Block diagram of the electronics (D = delay, T = trigger, C = coincidence, S = strobed coincidence).
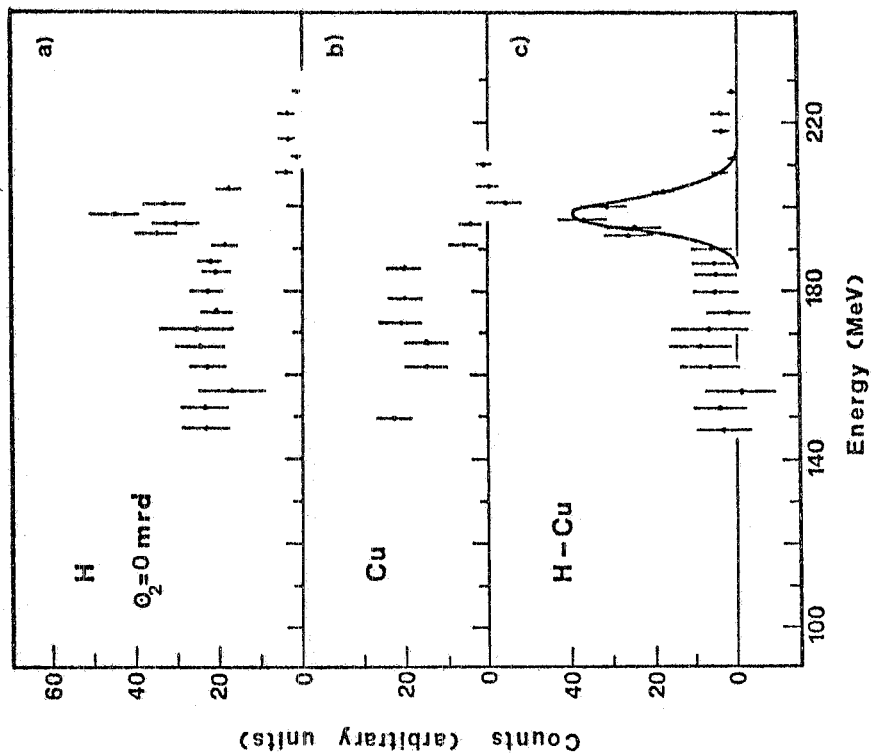
FIG. 7 – Photon energy spectrum at
$\theta_2 = 0.$ mrad.

FIG. 6 – Photon energy spectrum at
$\theta_1 = 17.5$ mrad.

experimental errors are due to poor statistics because the strong collimation, required by the spectrometer gap, cuts down drastically the photon beam intensity.

For thin radiators the number of annihilation and bremsstrahlung photons in the energy interval between k and k + dk is given by

$$\frac{dN_B}{dk} = \frac{t}{X_0} \frac{1}{k} F_B(E_0 \, kZ) \qquad\qquad \frac{dN_A}{dk} = \frac{t}{X_0} \frac{1}{Z} F_A(E_0 \, kZ)$$

where X_0 is the radiation length and t the thickness of the converter. F_B is a function calculated by Heitler[15], that takes into account the screening effect of the atomic electrons on the Coulomb field of the nucleus for photon energies away from the end point $(k/E_0 < 0.9)$ F_B is only weakly dependent on the atomic number Z. F_A describes the energy distribution of the annihilation photons[13] and is also almost independent from Z.

Different Z radiators having the same thickness in radiation length units will produce the same bremsstrahlung spectra as well as comparable multiple scattering effects[13], but annihilation peaks decreasing as $1/Z$.

We have performed measurements using H and Cu annihilation targets, each 0.011 radiation lenghts thick. The photon spectrum from the Cu target (Figs. 6b and 7b) shows a tipical bremsstrahlung energy dependence with a small amount of annihilation on the head. The H minus Cu difference spectra (Figs. 6c and 7c) correspond therefore to the contribution, only sligtly underestimated, of the annihilation photons in Hydrogen.

The annihilation photon spectrum from Hydrogen can be evaluated starting from the electromagnetic cross sections and taking into account all the target thickness effects, as described in ref. (14). The theoretical spectrum, corresponding to the geometrical set up of our experiment, has been folded with a gaussian resolution function of F. W. H. M. $\sim$ 9 MeV to take into account the finite spectrometer resolution. The final result, plotted as a continuous curve in Figs. 6c and 7c, shows a fairly good agreement between the theoretical and the experimental peaks.

A Montecarlo calculation of the spectrometer response function, presently in progress, taking into account the pair production differential cross section and the multiple scattering effects in the converter, shall afford a more detailed comparison of the theoretical and experimental spectra over the whole energy range of Figs. 6a and 7a. A preliminary evaluation of the convertion efficiency and solid angle shows that the measured photon intensity is also in fair agreement with the computed values (Table I).

10.

REFERENCES. -

(1) - J. Miller, C. Schuhl, G. Tamas and C. Tzara, J. Phys. Radium, 21, 296
     (1960); Nuclear Phys. 32, 236 (1962).
(2) - C. P. Jupiter, N. E. Hansen, R. E. Shafer and S. C. Fultz, Nuclear Instr.
     and Meth. 121, 866 (1961); C. R. Hatcher, R. L. Bramblett, N. E. Hansen
     and S. C. Fultz, Nuclear Instr. and Meth. 14, 337 (1961).
(3) - C. G. Schuhl, Les installations actuelles et futures pour l'etude des pro
     prietes nucleaires a energies intermediaires sur le site de Saclay,
     Proc. Intern. Conf. on Few Body Problems in Nuclear and Particle Phy-
     sics, Quebec (1974), pag. 788; Survey of monochromatic photon capabi
     lities, technologies and uses, Proc. Intern. Conf. on Fotonuclear Reac-
     tion and Applications, Asilomar (1973), pag. 1249; R. Bergere, Private
     Communication .
(4) - E. G. Fuller, Proc. Intern. Conf. on Photonuclear Reactions and Appli-
     cations, Asilomar (1973), pag. 1201.
(5) - D. Blum, J. Boucrot, B. Grossetête, W. Mc Gill and H. Nguyen Ngoc,
     Nuclear Instr. and Meth. 115, 553 (1974).
(6) - M. Sanzone, G. Ricco, S. Costa and L. Ferrero, Nuclear Phys. A153,
     401 (1970); S. Costa, Medium energy photoreaction, Proc. Intern. Conf.
     on Photonuclear Reaction and Applications, Asilomar (1973), pag. 1319.
(7) - P. Argan, G. Audit, N. De Botton, J. M. Laget, J. Martin, C. Schuhl and
     G. Tauras, Phys. Rev. Letters 29, 1191 (1972); P. Picozza, C. Schaerf,
     R. Scrimaglio, G. Goggi, A. Piazzoli and D. Scannicchio, Nuclear Phys.
     A 157, 190 (1970); Comptes rendue of the Rencontres de Saclay on Ef-
     fects mesoniques dans les noyaux, Saclay (1975).
(8) - G. P. Capitani, E. De Sanctis, S. Faini, C. Guaraldo, R. Malvano, G. Ric
     co, M. Sanzone e R. Scrimaglio, Frascati Report, LNF-72/99 (1972);
     G. P. Capitani, E. De Sanctis, S. Faini, C. Guaraldo, G. Ricco, M. Sanzo
     ne, R. Scrimaglio and A. Zucchiatti - Frascati Report, LNF Report (in press).
(9) - S. Tazzari, Private comunication.
(10) - S. N. Gardiner, J. L. Matthews and R. O. Owens, Nuclear Instr. and Meth.
     87, 285 (1970).
(11) - A. O. Komar, S. P. Kruglov and I. V. Lopatin, Nuclear Instr. and Meth.
     82, 125 (1970).
(12) - P. Benvenuto, D. Fabbri, E. Lodi Rizzini, L. Maiani, M. Napolitano,
     A. Piazza, V. Rossi, G. Susinno and L. Votano, Frascati Report LNF-
     -71/76 (1971).
(13) - J. L. Matthews and R. O. Owens, Nuclear Instr. and Meth. 91, 37 (1971).
(14) - E. Mancini and M. Sanzone, Nuclear Instr. and Meth. 66, 87 (1968).
(15) - U. Kneissl, E. A. Koop, G. Kuhl, K. H. Leister and A. Weller, Nuclear
     Instr. and Meth. 127, 1 (1975).
(16) - W. Heitler, The quantum theory of radiation, Clarendon Press Oxford
     1954.